The American Journal of Pathology, Vol. 171, No. 3, September 2007

DOI: 10.2353/ajpath.2007.061276

Cardiovascular, Pulmonary and Renal Pathology

Bone Marrow-Derived CXCR4$^+$ Cells Mobilized by Macrophage Colony-Stimulating Factor Participate in the Reduction of Infarct Area and Improvement of Cardiac Remodeling after Myocardial Infarction in Mice

Hajime Morimoto,* Masafumi Takahashi,† Yuji Shiba,† Atsushi Izawa,† Hirohiko Ise,† Minoru Hongo,‡ Kiyohiko Hatake,§ Kazuo Motoyoshi,¶ and Uichi Ikeda*†

From the Department of Cardiovascular Medicine and Regeneration and the Division of Cardiovascular Sciences,† the Department of Organ Regeneration, Shinshu University Graduate School of Medicine, Matsumoto; the Department of Cardiovascular Medicine,‡ Shinshu University School of Health Sciences, Matsumoto; the Cancer Chemotherapy Center,§ Japanese Foundation for Cancer Research, Tokyo; and the Third Department of Internal Medicine,¶ National Defense Medical College, Saitama, Japan*

The monocyte/macrophage lineage might affect the healing process after myocardial infarction (MI). Because macrophage colony-stimulating factor (M-CSF) stimulates differentiation and proliferation of this lineage, we examined the effect of M-CSF treatment on infarct size and left ventricular (LV) remodeling after MI. MI was induced in C57BL/6J mice by ligation of the left coronary artery. Either recombinant human M-CSF or saline was administered for 5 consecutive days after MI induction. M-CSF treatment significantly reduced the infarct size ($P < 0.05$) and scar formation ($P < 0.05$) and improved the LV dysfunction (percent fractional shortening, $P < 0.001$) after the MI. Immunohistochemistry revealed that M-CSF increased macrophage infiltration (F4/80) and neovascularization (CD31) of the infarct myocardium but did not increase myofibroblast accumulation (α-smooth muscle actin). M-CSF mobilized CXCR4$^+$ cells into peripheral circulation, and the mobilized CXCR4$^+$ cells were then recruited into the infarct area in which SDF-1 showed marked expression. The CXCR4 antagonist AMD3100 deteriorated the infarction and LV function after the MI in the M-CSF-treated mice. In conclusion, M-CSF reduced infarct area and improved LV remodeling after MI through the recruitment of CXCR4$^+$ cells into the infarct myocardium by the SDF-1-CXCR4 axis activation; this suggests that the SDF-1-CXCR4 axis is as a potential target for the treatment of MI. ***(Am J Pathol 2007, 171:755–766; DOI: 10.2353/ajpath.2007.061276)***

Myocardial infarction (MI) is accompanied by inflammatory responses that lead to the recruitment of leukocytes and subsequent myocardial damage, healing, and scar formation. The recruitment and activation of monocytes/macrophages in the infarct myocardium have been shown to play an important role in the processes that occur after MI. The activated macrophages lead to the release of cytokines and proteinases that can induce further inflammation and left ventricular (LV) remodeling. Furthermore, recent evidence indicates that some endothelial progenitor cells (EPCs) are derived from cells of the monocytic lineage and participate in the neovascularization of ischemic tissues.[1–3] These cells have also been reported to secrete a large amount of angiogenic factors such as the vascular endothelial growth factor and the hepatocyte growth factor[3]; this suggests that monocytes/macrophages could influence LV dysfunction and remodeling after MI.

Supported by research grants from the Ministry of Health, Labor and Welfare of Japan (Research on Measures for Intractable Diseases, to M.T. and U.I.) and the Ministry of Education, Science, Sports and Culture of Japan (to M.T. and U.I.).

Supplemental material for this article can be found on *http://ajp.amjpathol.org.*

Accepted for publication May 16, 2007.

Address reprint requests to Masafumi Takahashi, M.D., Ph.D., Division of Cardiovascular Sciences, Department of Organ Regeneration, Shinshu University Graduate School of Medicine, 3-1-1 Asahi, Matsumoto, Nagano 390-8621, Japan. E-mail: masafumi@sch.md.shinshu-u.ac.jp.

The macrophage colony-stimulating factor (M-CSF) is a multifunctional proinflammatory cytokine that regulates the differentiation, proliferation, and survival of monocytic progenitor cells[4] and plays a role in various processes involved in inflammatory diseases. Furthermore, it has been recently demonstrated that M-CSF is expressed by nonhematopoietic cells such as endothelial cells, smooth muscle cells, and cardiomyocytes and that its function extends beyond its role in monocytic progenitor cells. A recent investigation demonstrated that M-CSF is expressed in the infarct heart and plays an important role in myocardial healing postinfarction.[5] However, the effect of M-CSF on cardiac dysfunction and remodeling after MI is not entirely understood. In the present study, we demonstrate that exogenous M-CSF treatment induces macrophage infiltration and capillary formation in the infarct myocardium, thereby improving LV dysfunction and remodeling. This process is mediated through a system that comprises a key stem cell homing factor, the stromal cell-derived factor (SDF-1/CXCL12), and the SDF-1 receptor CXCR4. The findings of this study may provide new insights into the role of M-CSF and the SDF-1-CXCR4 axis in the pathophysiology of MI.

Materials and Methods

Animals

All mice (C57BL/6J, male) were purchased from Japan SLC Inc. (Hamamatsu, Japan). Their ages ranged from 8 to 12 weeks. Mice were fed a standard diet and water and maintained on a 12-hour light/dark cycle. All of the experiments in this study were performed in accordance with the Shinshu University Guide for Laboratory Animals, which conforms to the National Institutes of Health Guidelines.

Experimental Protocols

In the preliminary experiments, we examined the effect of M-CSF (5, 50, and 500 μg/kg, i.p.) on the number of peripheral monocytes in C57BL/6J mice. We found that the administration of 500 μg/kg of recombinant human M-CSF (kindly provided by Morinaga Milk Industry Co. Ltd., Kanagawa, Japan) significantly increased the number of peripheral monocytes; this finding was consistent with a previous report.[6] Therefore, in the present study, we used this M-CSF at a dose of 500 μg/kg per day. We also used recombinant human granulocyte colony-stimulating factor (G-CSF; kindly provided by Chugai Pharmaceutical, Co. Ltd., Tokyo, Japan) at a dose of 100 μg/kg per day.

The mice were anesthetized with an intraperitoneal injection of 50 mg/kg pentobarbital sodium and splenectomized, not only to eliminate spleen-derived stem cells (eg, EPCs and $CXCR4^+$ cells) but also to prevent the homing of bone marrow-derived stem cells to the spleen.[7] The animals were allowed to recover for 14 days, after which MI was induced. Either recombinant human M-CSF (i.p., $n = 60$), G-CSF (s.c., $n = 12$), or saline (i.p., vehicle, $n = 53$) was administered to the splenectomized mice for 5 consecutive days after MI induction. The M-CSF treatment was well tolerated, and no abnormal behavior was observed. AMD3100 (Sigma, St. Louis, MO) was administered subcutaneously at a concentration of 300 μg/kg per hour for 7 days after the MI by using a micro-osmotic pump (Alzet model 1007D; Durect Corporation, Cupertino, CA).

MI Induction Protocol

A murine model of MI was constructed as described previously.[8] Intubation was performed after anesthetizing the mice with isoflurane. The mice were ventilated with a rodent ventilator (MiniVent Type 845; Harvard Apparatus, Holliston, MA). A left thoracotomy was performed through the fourth or fifth intercostal space. An 8-0 nylon suture was placed directly beneath the left atrium in the interventricular groove. Successful coronary occlusion was verified by observing the development of a pale color in the distal myocardium after the ligation of the left coronary artery. The lungs were re-expanded using positive pressure at end expiration, and the thoracotomy and skin incision were closed with a 3-0 silk suture. Extubation was performed when spontaneous respiration resumed.

Histology and Immunohistochemistry

Histological and immunohistochemical analyses were performed as described previously.[9] In brief, the mice were euthanized after irrigation with saline (Otsuka Pharmaceutical Co. Ltd., Tokushima, Japan), and their blood was completely washed out. The hearts were embedded in optimal cutting temperature compound (Tissue-Tek, Sakura Finetechnical Co. Ltd., Tokyo, Japan) and frozen on dry ice. They were then sectioned transversely from the apex to the site of ligation beneath the left atrium. Tissue sections (10-μm thick) were cut on a cryostat (CM-1900; Leica Microsystems GmbH, Wetzlar, Germany) and histologically examined. Four sections were selected from each heart to perform morphometrical assessments of the LV myocardium and the infarct size. The sections were stained with hematoxylin-eosin (H&E) and Masson's trichrome. Measurements were performed using Scion Image software (Beta 4.03; Scion Corporation, Frederick, MD). The infarct size was calculated as a percentage of the total LV area. The extent of fibrosis in the sections was measured, and the value was expressed as the ratio of the Masson's trichrome-stained area to the total LV free wall area.

For immunohistochemical analysis, the heart sections were incubated with primary antibodies against M-CSF (kindly provided by Morinaga Milk Industry Co. Ltd.), mouse CD31 (clone MEC13.3, BD Bioscience, San Jose, CA), F4/80 (clone A3-1; RDI, Flanders, NJ), α-smooth muscle actin (α-SMA; clone 1A4; Sigma), and CD184 (CXCR4, clone 2B11; BD Biosciences). This was followed by incubation with biotin-conjugated secondary antibodies. The sections were washed and treated with avidin peroxidase (ABC kit; Vector Laboratories, Burlingame, CA), and the stain was developed using the 3,3′-diaminobenzidine (DAB) substrate kit (Vector Laboratories). The sections were then counterstained with hematoxylin.

Mouse on mouse (M.O.M.) basic kits (Vector Laboratories) were used to specifically localize mouse primary monoclonal antibodies in the tissues. No signal was detected when an irrelevant IgG was used as the negative control instead of the primary antibody. All of the measurements were performed in a double-blind manner by two independent researchers.

Cell Cultures and Hypoxia-Reoxygenation

Primary cultures of murine neonatal cardiomyocytes and cardiac fibroblasts were prepared and cultured as described previously.[8] For hypoxia-reoxygenation experiments, cells were exposed to hypoxia induced with AnaeroPack (Mitsubishi Gas Chemical, Tokyo, Japan) for 6 hours, followed by reoxygenation for 18 hours.

Flow Cytometric Analysis

Blood samples were collected from the mice at baseline, 7 days, and 14 days after the MI. Circulating cells were identified using a nucleated cell fraction. The nucleated cells were double-labeled with the following antibodies: peridinin chlorophyll protein-conjugated anti-CD11b (Mac-1, clone M1/70; BD Biosciences), fluorescein isothiocyanate-conjugated anti-Ly-6G (Gr-1, clone 1A8), fluorescein isothiocyanate-conjugated anti-CD34 (clone RAM34; BD Biosciences), phycoerythrin-conjugated anti-Flk-1 (VEGFR2/KDR, clone Avas 12a1; BD Biosciences), and phycoerythrin-conjugated anti-CXCR4 (clone 2B11; BD Biosciences). For staining with antibody against α-SMA, cells were permeabilized with Cytofix/Cytoperm (BD Biosciences) according to the manufacturer's instructions. The cells were examined by flow cytometry (FACSCalibur; Becton Dickinson) and analyzed using CellQUEST software version 3.3 (Becton Dickinson).

Serum Levels of Inflammatory Cytokines

The serum levels of monocyte chemoattractant protein-1 (MCP-1), interleukin (IL)-6, IL-10, IL-12p70, interferon-γ (IFN-γ), and tumor necrosis factor-α (TNF-α) were assessed using the CBA Mouse Inflammation Kit (BD Biosciences) according to the manufacturer's instructions.

Echocardiography

Transthoracic echocardiography was performed at baseline, 7 days, and 14 days after the MI by using a Vivid Five system (GE Yokogawa Medical Systems, Tokyo, Japan) as described previously.[10] Ketamine (50 mg/kg) and xylazine (10 mg/kg) were administered intraperitoneally for mild sedation. Two-dimensional targeted M-mode echocardiograms were obtained along the short axis of the left ventricle at the level of the papillary muscles, and at least three consecutive beats were evaluated. The phases in which the smallest and largest area of the left ventricle were obtained were defined as the left ventricular end-systolic diameter (LVESD) and left ventricular end-diastolic diameter (LVEDD), respectively. The percentage fractional shortening (%FS) was calculated using the standard formula: $\%FS = [(LVEDD - LVESD)/LVEDD] \times 100$. All measurements were performed in a double-blind manner by two independent researchers.

Real-Time Reverse Transcription-Polymerase Chain Reaction Analysis

Total cellular RNA was extracted using ISOGEN (Nippon Gene Co. Ltd., Toyama, Japan) or RNA-Bee (Tel-Test, Inc., Friendswood, TX), according to the manufacturer's instructions. Real-time reverse transciption-polymerase chain reaction (RT-PCR) analysis was performed by using the ABI Prism 7000 system (Applied Biosystems, Inc.) to detect the mRNA expression of c-fms, G-CSF receptor (G-CSFR), collagen type I and type III, transforming growth factor-β1 (TGF-β1), and β-actin.[11] The following primers (oligonucleotide sequences are provided in parentheses in the order of antisense and sense primers) were used: c-fms (5′-CATGGCCTTCCTTGCTTCTAA-3′ and 5′-ACATGTCCGCTGGTCAACAG-3′), G-CSFR (5′-GTCCAGCGAGTCCCCAAAG-3′ and 5′-AGCATGGGAGGCTCCAATT-3′), collagen type I (5′-CGGAGAAGAAGGAAAACGAGGAG-3′ and 5′-CACCATCAGCACCAGGGAAAC-3′), collagen type III (5′-CCCAA CCCAGAGATCCCATT-3′ and 5′-GAAGCACAGGAGCA GGTGTAGA-3′), TGF-β1 (5′-GCAACATGTGGAACTCTACCAGA-3′ and 5′-GACGTCAAAAGACAGCCACTCA-3′), and β-actin (5′-CCTGAGCGCAAGTACTCTGTGT-3′ and 5′-GCTGATCCACATCTGCTGGAA-3′). The expression levels of each target gene were normalized by subtracting the corresponding β-actin threshold cycle (C_T) values; this was done by using the $\Delta\Delta C_T$ comparative method.

Apoptosis Assessment

Apoptotic cells were identified by the terminal deoxynucleotidyl transferase dUTP nick-end labeling staining kit (Roche Diagnostics, Mannheim, Germany) performed according to the manufacturer's instructions.

Statistical Analysis

Data are represented as mean ± SEM. Multiple group comparison was performed by one-way analysis of variance (analysis of variance), followed by Scheffé's F-test for comparison of the means. The comparison between two groups was analyzed by an F-test, followed by a two-tailed *t*-test. Values of $P < 0.05$ were considered statistically significant.

Results

Expression of M-CSF in the Myocardium after MI Induction

First, we examined whether the expression of M-CSF was up-regulated in the infarct area after the permanent MI.

Although no M-CSF expression was visualized in the infarct myocardium and vasculatures at baseline, immunohistochemical analysis revealed that the M-CSF expression was clearly up-regulated in these regions 6 to 24 hours after the MI, and it declined 3 to 7 days after the MI (Figure 1A). To identify the cell types that express M-CSF, double-immunohistological staining using antibodies against M-CSF and the cardiac-specific marker cTnI or the endothelial marker CD31 was performed. We detected the coexpression of M-CSF and cTnI, but not that of CD31 (Figure 1B). By using RT-PCR, we further examined whether cardiomyocytes express M-CSF mRNA and observed the expression of M-CSF mRNA in the murine heart and cultured cardiomyocytes (Figure 1C). The J774 cell line was used as a positive control for M-CSF expression. These findings suggest that M-CSF plays a role in the processes involved in MI.

Effect of M-CSF or G-CSF on the Infarct Area and Scar Formation

Next, we examined the effect of exogenous M-CSF treatment on the infarct area and scar formation after the MI. As shown in Figure 2, A and B, the infarct area at 14 days after MI in the M-CSF-treated mice decreased significantly compared with that in the vehicle-treated mice ($P < 0.01$). Further, Masson's trichrome staining demonstrated that scar formation was significantly reduced in the former compared with that in the latter ($P < 0.05$) (Figure 2, C and D). In addition, because the G-CSF has been shown to improve LV dysfunction and remodeling after MI,[12,13] we tested the effect of G-CSF and confirmed that G-CSF treatment significantly reduced the infarct area and scar formation after the MI (Figure 2). We also assessed the infarct area at the early stage after MI and showed that M-CSF treatment appeared to decrease the infarct area on days 3 and 7 after the MI (Supplemental Figure 1 at *http://ajp.amipathol.org*).

Further, we assessed the LV function after the MI by using echocardiography. No significant difference was observed in the %FS between the vehicle- and M-CSF-treated mice at baseline. In the vehicle-treated mice, a marked decrease in the %FS was observed 7 days after MI, and this decrease was sustained for 28 days. In contrast, the %FS was maintained in the M-CSF-treated mice after the MI (Table 1; 14 days, vehicle: 25.8 ± 1.0% versus M-CSF: 33.5 ± 0.8%, $P < 0.001$). As expected, the %FS was also maintained in the G-CSF-treated mice after the MI (14 days, G-CSF: 34.4 ± 0.5%, $P < 0.001$ versus vehicle).

Expression of c-fms and G-CSFR in the Myocardium

A previous investigation reported that G-CSF directly activates the Jak-Stat pathway via the G-CSFR in cardiomyocytes and exerts cardioprotective effects.[12] Therefore, we examined the expression of the M-CSF receptor c-fms and G-CSFR in the myocardium after the MI. Real-time RT-PCR analysis revealed that c-fms

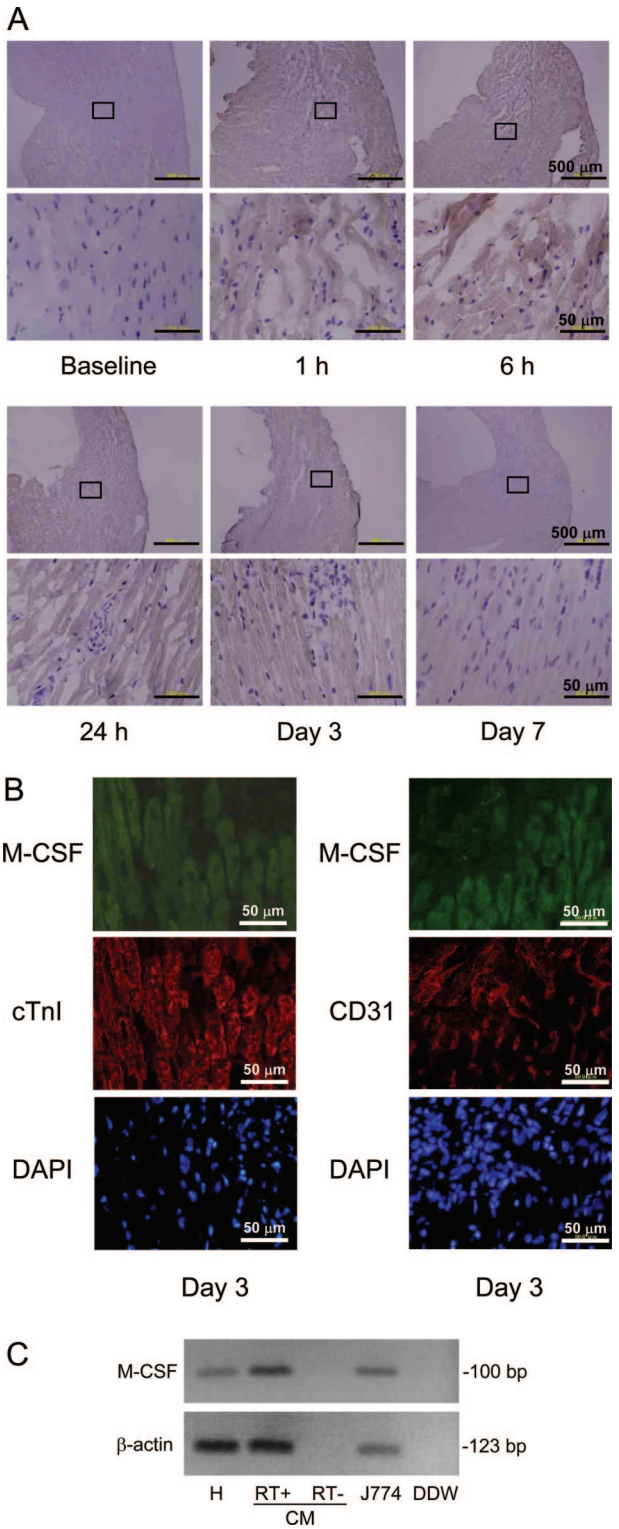

Figure 1. Expression of M-CSF in the myocardium after MI induction. **A** and **B:** Heart sections were obtained from the mice at baseline, 1 hour, 6 hours, 24 hours, 3 days, and 7 days after MI; these sections were immunohistochemically analyzed by staining with anti-M-CSF antibodies (**A**). Double-immunohistochemical staining for M-CSF (green) and cTnI or CD31 (red) was performed (**B**). Further, nucleic acid was stained with 4,6-diamidino-2-phenylindole (DAPI). The representative photographs are shown ($n = 3$). **C:** Total RNA was extracted from the murine heart (H), cultured cardiomyocytes (CM), and J774 cell line and analyzed for M-CSF and β-actin by RT-PCR analysis. DDW, deionized distilled water.

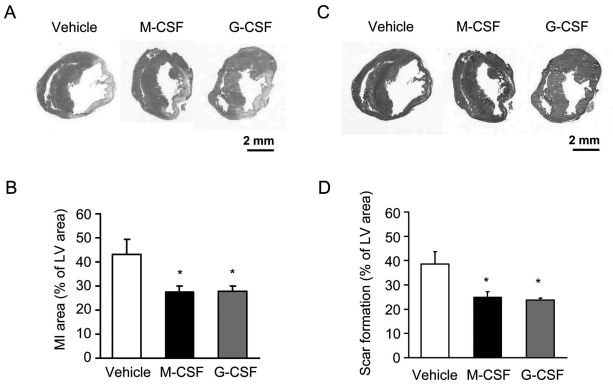

Figure 2. Effect of M-CSF or G-CSF on MI area and scar formation. **A** and **C:** Heart sections were obtained from the vehicle-, M-CSF-, and G-CSF-treated mice at 14 days after the MI, and these were stained with H&E (**A**) and Masson's trichrome (**C**). **B** and **D:** Bar graphs indicate the MI area (**B**) and scar formation (**D**). Results are expressed as mean ± SEM (each $n = 10$). $^{*}P < 0.05$ versus vehicle.

expression was decreased by 43% at 6 hours after the MI, and this decrease was sustained for at least 7 days (Figure 3A). In contrast, G-CSFR expression was increased at 6 hours after the MI and reached a peak at 24 hours (approximately 22-fold expression; Figure 3B). Immunohistochemical staining showed the decreased expression of c-fms protein in the heart at 6 hours after the MI (Figure 3C). These results suggest that M-CSF might improve LV dysfunction and remodeling after MI via its effect on monocytes/macrophages rather than that on cardiomyocytes.

Macrophage Infiltration and Endothelial Cell Density

To investigate the mechanism underlying the beneficial effect of M-CSF, we performed an immunohistochemical analysis to detect macrophages (F4/80) and endothelial cells (CD31). The number of infiltrated macrophages in the infarct area of the heart was greater in the M-CSF-treated mice than in the vehicle-treated mice after the MI ($P < 0.001$, Figure 4, A and B). The density of endothelial cells that was determined by CD31 expression increased significantly in the M-CSF-treated mice compared with

Table 1. Echocardiographic Findings in Vehicle and M-CSF-Treated Mice after MI Induction

	Baseline	Day 7	Day 14	Day 21	Day 28
Vehicle					
n	24	24	23	6	6
B.W. (g)	25.1 ± 0.3	24.8 ± 0.5	26.0 ± 0.4	28.3 ± 0.2**	28.5 ± 0.3**
B.W. (%)	100	98.8 ± 0.9	102.5 ± 0.9	107.6 ± 2.0**	108.3 ± 2.0**
IVSd (mm)	0.74 ± 0.02	0.67 ± 0.03	0.65 ± 0.03	0.60 ± 0.02	0.55 ± 0.05*
LVDd (mm)	4.04 ± 0.11	4.45 ± 0.10	4.92 ± 0.12**	5.13 ± 0.17**	5.22 ± 0.21**
LVPWd (mm)	0.82 ± 0.03	0.90 ± 0.05	0.85 ± 0.04	0.71 ± 0.02	0.73 ± 0.04
IVSs (mm)	1.36 ± 0.03	1.12 ± 0.04**	1.04 ± 0.04**	1.02 ± 0.03**	0.99 ± 0.04**
LVDs (mm)	2.24 ± 0.07	3.20 ± 0.08**	3.66 ± 0.12**	3.71 ± 0.14**	3.83 ± 0.18**
LVPWs (mm)	1.44 ± 0.02	1.27 ± 0.05**	1.23 ± 0.03**	1.07 ± 0.03**	1.08 ± 0.02**
FS (%)	44.9 ± 0.7	28.2 ± 0.9**	25.8 ± 1.0**	27.6 ± 0.7**	26.7 ± 1.0**
FS (% of baseline)	100	63.2 ± 2.1**	58.8 ± 2.3**	64.2 ± 1.7**	61.9 ± 1.9**
M-CSF					
n	25	25	23	5	5
B.W. (g)	24.8 ± 0.3	24.2 ± 0.6	25.2 ± 0.4	27.8 ± 0.6	28.3 ± 0.7*
B.W. (%)	100	97.4 ± 1.9	101.3 ± 0.9	105.2 ± 1.2	107.0 ± 1.2
IVSd (mm)	0.71 ± 0.02	0.68 ± 0.02	0.67 ± 0.02	0.64 ± 0.02	0.63 ± 0.04
LVDd (mm)	4.10 ± 0.06	4.52 ± 0.06**	4.78 ± 0.11**	4.97 ± 0.26**	5.14 ± 0.19**
LVPWd (mm)	0.80 ± 0.02	0.79 ± 0.03	0.80 ± 0.02	0.72 ± 0.05	0.70 ± 0.04
IVSs (mm)	1.29 ± 0.02	1.18 ± 0.03	1.19 ± 0.03††	1.12 ± 0.05	1.13 ± 0.09
LVDs (mm)	2.32 ± 0.05	3.03 ± 0.06**	3.18 ± 0.09**,††	3.22 ± 0.18**	3.44 ± 0.14**
LVPWs (mm)	1.42 ± 0.02	1.28 ± 0.04*	1.36 ± 0.03††	1.24 ± 0.04††	1.17 ± 0.05*
FS (%)	43.6 ± 0.6	32.9 ± 0.8**,†††	33.5 ± 0.8**,†††	35.2 ± 0.8**,†††	32.9 ± 1.4**,††
FS (% of baseline)	100	75.9 ± 2.1**,†††	76.7 ± 2.3**,†††	83.1 ± 1.8**,†††	77.7 ± 3.4**,††
G-CSF					
n	12	10	10		
B.W. (g)	24.9 ± 0.3	24.0 ± 0.3	24.8 ± 0.3†		
B.W. (%)	100	96.3 ± 1.4**	100.3 ± 0.5		
IVSd (mm)	0.71 ± 0.04	0.77 ± 0.02†	0.72 ± 0.04		
LVDd (mm)	4.06 ± 0.09	4.68 ± 0.23*	5.04 ± 0.15**		
LVPWd (mm)	0.81 ± 0.06	1.08 ± 0.12	0.98 ± 0.08		
IVSs (mm)	1.27 ± 0.04	1.31 ± 0.04††	1.37 ± 0.04†††		
LVDs (mm)	2.32 ± 0.06	3.02 ± 0.19**	3.31 ± 0.10**,†		
LVPWs (mm)	1.40 ± 0.04	1.59 ± 0.08††	1.57 ± 0.08††		
FS (%)	42.9 ± 0.5	35.9 ± 1.5**,†††	34.4 ± 0.5**,†††		
FS (% of baseline)	100	83.4 ± 3.0**,†††	80.5 ± 1.8**,†††		

Data represent the mean S.E.M. *n*, number: B.W., body weight; IVSd, interventricular septal diastolic thickness; LVDd, left ventricular diastolic dimension; LVPWd, left ventricular posterior wall idastolic thickness; IVSs, interventricular septal systolic thickness; LVDs, left ventricular systolic dimension; LVPWs, left ventricular posterior wall systolic thickness; FS, fractional shortening.

* $P < 0.05$ and ** $P < 0.01$ versus baseline.

† $P < 0.05$, †† $P < 0.01$, and ††† $P < 0.001$ versus vehicle.

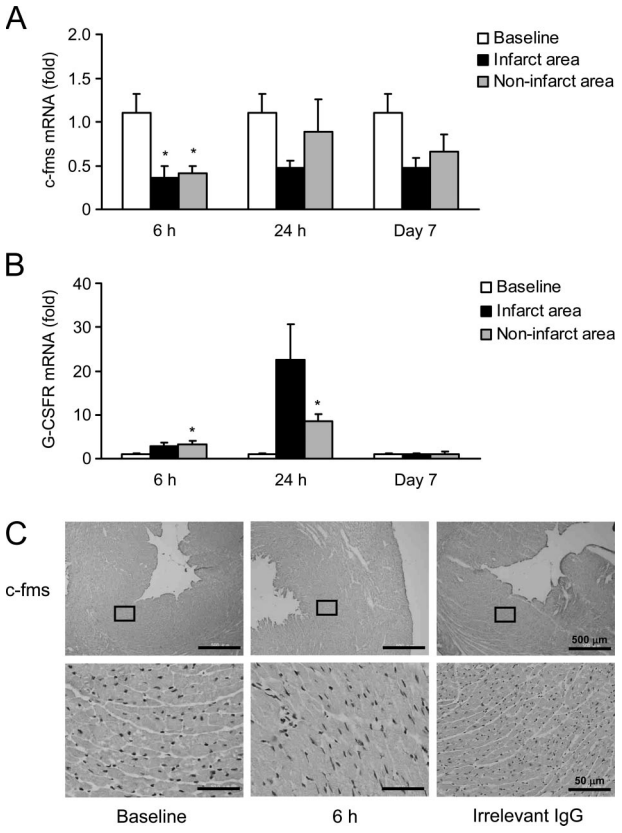

Figure 3. Expression of c-fms and G-CSFR in the myocardium. **A** and **B:** Total RNA was extracted from the infarct and noninfarct areas of the heart at baseline (sham operation), 6 hours, 24 hours, and 7 days after the MI and analyzed for c-fms (**A**) or G-CSFR (**B**) by real-time RT-PCR analysis. Results are expressed as mean ± SEM (each $n = 5$). $^{*}P < 0.05$ versus baseline. **C:** Heart sections were obtained from the mice at baseline and 6 hours after MI; these sections were immunohistochemically analyzed by staining with anti-c-fms antibody. Irrelevant IgG was used as a negative control.

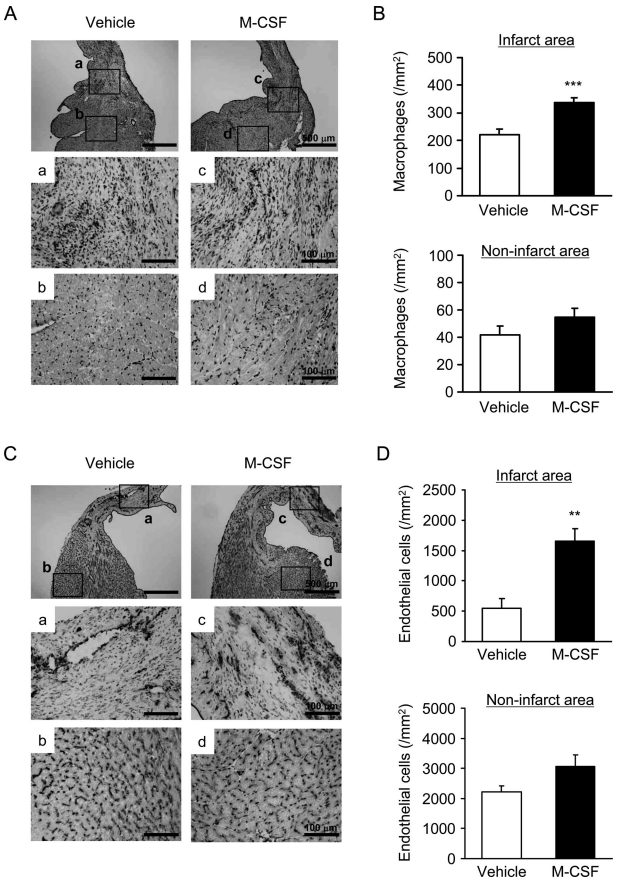

Figure 4. Macrophage infiltration and endothelial cell density. **A** and **C:** Heart sections were obtained from the vehicle- or M-CSF-treated mice 14 days after MI; these sections were immunohistochemically analyzed by staining with F4/80 (macrophages; **A**) and anti-CD31 antibody (endothelial cells; **C**). **B** and **D:** Bar graphs indicate the number of macrophages (**B**) and endothelial cells (**D**) in the infarct (**a** and **c**) and noninfarct areas (**b** and **d**). Results are expressed as mean ± SEM (each $n = 5$). $^{**}P < 0.01$, and $^{***}P < 0.001$ versus vehicle.

that in the vehicle-treated mice ($P < 0.01$, Figure 4, C and D). These findings suggest that M-CSF treatment promotes macrophage infiltration and neovascularization in the infarct myocardium.

Effect of M-CSF on Differentiation into Myofibroblasts and Cardiomyocyte Apoptosis

Cardiac fibroblasts have been shown to differentiate into myofibroblasts during the process of myocardial repair and remodeling after MI.[14] Because myofibroblasts are characterized by the presence of α-SMA, immunohistochemical analysis of α-SMA was performed. The number of α-SMA-positive myofibroblasts was notably increased at the infarct area compared with that at the noninfarct area (Figure 5, A and B). However, no change was observed in the number of myofibroblasts in the M-CSF-treated mice compared with that in the vehicle-treated mice ($P = 0.245$).

To examine the effect of M-CSF on the differentiation into myofibroblasts *in vitro*, we used murine neonatal cardiac fibroblasts. M-CSF accelerated the *in vitro* differentiation of cardiac fibroblasts into myofibroblasts (Figure 5C). We performed flow cytometry analysis to quantify this differentiation. Interestingly, M-CSF clearly stimulated the *in vitro* differentiation of not only cardiac fibroblasts but also peripheral blood cells and bone marrow-derived cells (Figure 5, D and E).

To assess the involvement of apoptosis after MI in the vehicle- and M-CSF-treated mice, terminal deoxynucleotidyl transferase dUTP nick-end labeling staining was performed; however, no differences were found in the number of apoptotic cells between the vehicle- and M-CSF-treated mice (Supplemental Figure 2A at *http://ajp. amipathol.org*). To investigate further whether M-CSF confers an anti-apoptotic effect on cardiomyocytes, *in vitro* experiments using murine cultured cardiomyocytes were performed. We exposed cardiomyocytes to hypoxia-reoxygenation in the absence or presence of M-CSF and examined cardiomyocyte apoptosis. Treatment with M-CSF reduced the number of apoptotic cells induced by hypoxia-reoxygenation compared with cells that were not treated with M-CSF (Supplemental Figure 2B at *http://ajp. amipathol.org*).

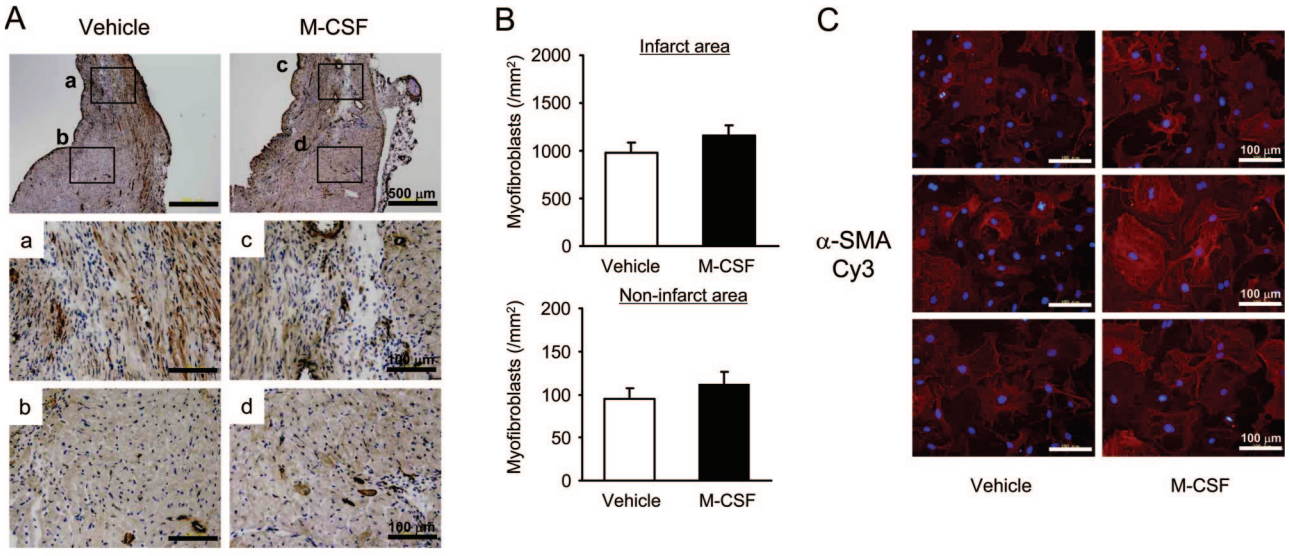

Figure 5. Effect of M-CSF on *in vitro* differentiation into myofibroblasts. **A:** Heart sections were obtained from the vehicle- or M-CSF-treated mice 14 days after MI; these sections were immunohistochemically analyzed by staining with anti-α-SMA antibody (myofibroblasts). **B:** Bar graphs indicate the number of myofibroblasts in the infarct (**a** and **c**) and noninfarct areas (**b** and **d**). **C:** Cardiac fibroblasts were treated with vehicle or M-CSF (10 ng/ml) for 24 hours and then stained with α-SMA (red: α-SMA, blue: 4,6-diamidino-2-phenylindole). **D** and **E:** Peripheral blood cells (PB), bone marrow cells (BM), and cardiac fibroblasts were treated with vehicle or M-CSF (10 ng/ml) for 24 hours, stained with α-SMA, and then analyzed by flow cytometry. Irrelevant IgG was used as a negative control. The results are representative of three independent experiments.

Involvement of Inflammatory Cytokines, Collagen, and TGF-β1

To investigate whether cytokines and collagen synthesis are involved in reducing the infarct area and scar formation after MI, we determined the serum level of MCP-1, IL-6, IL-10, IL-12p70, IFN-γ, and TNF-α. Serum IL-6 and MCP-1 levels tended to increase 24 hours after the MI (Figure 6, A and B), whereas no increase was observed in the IL-12p70 level (Figure 6C). The other inflammatory cytokines were under detectable limits (<20 pg/ml, data not shown). Real-time RT-PCR analysis revealed that the mRNA expression of collagen type I and type III was clearly up-regulated in the infarct area of the vehicle- and M-CSF-treated mice 14 days after the MI, and no difference was observed in these expression levels between the two groups (Figure 6, D and E). In addition, no significant increase was observed in the TGF-β1 mRNA expression in the infarct area (Figure 6F).

Mobilization of Bone Marrow-Derived Cells

To determine the types of bone marrow-derived cells that were mobilized by M-CSF treatment, we assessed the percentage of Mac-1^+/Gr-1^- cells (monocytic marker), $CD34^+$/Flk-1^+ cells, and $CXCR4^+$ cells. Flow cytometric analysis revealed that M-CSF treatment resulted in a significant increase in the Mac-1^+/Gr-1^- ($P < 0.05$) and $CXCR4^+$ cells ($P < 0.01$) but not in the $CD34^+$/Flk-1^+ cells in peripheral circulation 72 hours after the MI (Figure 7, A–C). Furthermore, M-CSF treatment preferentially increased the Mac-1^+/$CXCR4^+$ cells (Figure 7D).

Involvement of the SDF-1-CXCR4 Axis

Because the peripheral $CXCR4^+$ cells were observed to increase substantially in the M-CSF-treated mice after the MI, we performed an immunohistochemical analysis to detect CXCR4 and its ligand SDF-1. The expression of SDF-1 was predominantly observed in the infarct and border areas but not in the noninfarct area (Figure 8A).

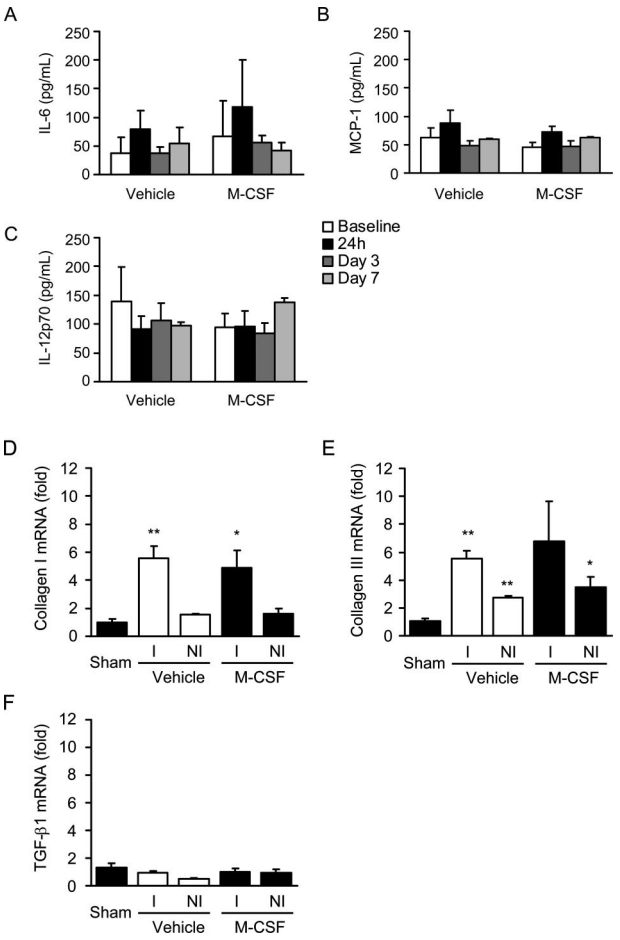

Figure 6. Involvement of inflammatory cytokines, collagen, and TGF-β1. **A–C:** Blood samples were obtained from the vehicle- or M-CSF-treated mice at baseline, 24 hours, 3 days, and 7 days after the MI. Serum levels of IL-6 (**A**), MCP-1 (**B**), and IL-12p70 (**C**) were assessed. Data are represented as mean ± SEM ($n = 5$). **D–F:** Total RNA was extracted from the infarct (I) or noninfarct (NI) area in the sham-operated, vehicle-, and M-CSF-treated mice 14 days after the MI and analyzed for collagen type I, collagen type III, and TGF-β1 mRNA expression by real-time RT-PCR analysis. Results are expressed as mean ± SEM ($n = 3$). $^{*}P < 0.05$, and $^{**}P < 0.01$ versus sham.

No difference was observed in the levels of SDF-1 expression between the vehicle- and M-CSF-treated mice. Similarly, the number of infiltrated CXCR4$^+$ cells increased in the infarct and border areas but not in the noninfarct area (Figure 8B). Quantitative analysis revealed that M-CSF treatment significantly increased the number of CXCR4$^+$ cells increased in the border area of MI mice (Figure 8C, $P < 0.01$).

To explore the role of the SDF-1-CXCR4 axis, we used a novel CXCR4 antagonist, namely, AMD3100. AMD3100 was administered subcutaneously for 7 consecutive days after the MI by using a micro-osmotic pump. The administration of AMD3100 significantly increased the number of circulating white blood cells, particularly neutrophils (data not shown); this finding was consistent with that in previous reports.[15] As shown in Figure 8, D–F, M-CSF treatment improved LV function at 7 and 14 days after the MI, and additional treatment with AMD3100 deteriorated the infarction ($P = 0.054$) and LV function ($P < 0.05$) in the M-CSF-treated mice.

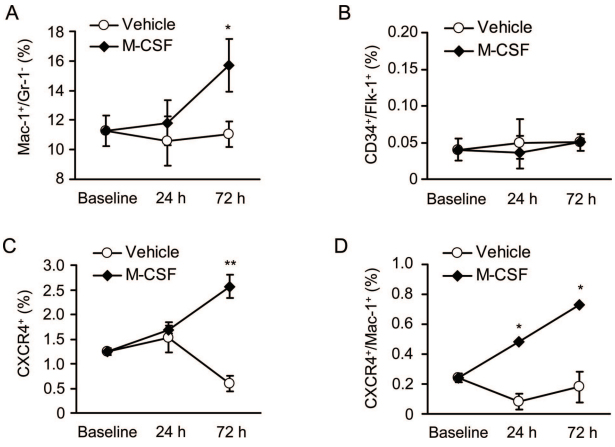

Figure 7. Mobilization of bone marrow-derived cells. **A–D:** Blood samples were collected from the vehicle- or M-CSF-treated mice at baseline, 24 hours, and 72 hours after the MI. The percentage of Mac-1$^+$/Gr-1$^-$, CD34$^+$/Flk-1$^+$, and CXCR4$^+$ cells was assessed by flow cytometric analysis. Results are expressed as mean ± SEM ($n = 3$). $^{*}P < 0.05$, and $^{**}P < 0.01$ versus vehicle.

Discussion

The major findings of this study are as follows: i) M-CSF expression was up-regulated in the infarct myocardium; ii) M-CSF treatment reduced the infarct size and scar formation and improved LV dysfunction and remodeling after the MI; iii) c-fms expression decreased in the infarct myocardium; iv) M-CSF treatment also induced macrophage infiltration and capillary formation but not myofibroblast accumulation in the infarct area; v) M-CSF treatment mobilized the number of CXCR4$^+$ cells in peripheral circulation; vi) SDF-1 expression was marked in the infarct myocardium, and CXCR4$^+$ cells were recruited to the infarct area in the M-CSF-treated mice; and vii) the CXCR4 antagonist AMD3100 deteriorated the infarction and LV function after the MI in the M-CSF-treated mice. These findings suggest that M-CSF reduces infarct size and scar formation and improves LV dysfunction and remodeling after the MI via the activation of SDF-1-CXCR4 axis.

Effect of M-CSF Treatment on the Infarct Area and LV Dysfunction after the MI

Increasing evidence indicates the importance of bone marrow-derived stem/progenitor cells in the pathophysiology of cardiovascular diseases. In particular, bone marrow stem cells could promote neovascularization and cardiac regeneration after MI and thereby improve LV dysfunction and remodeling[16,17]; this suggests the therapeutic potential of bone marrow stem cell transplantation for the treatment of cardiovascular diseases. Because colony-stimulating factors could mobilize bone marrow stem cells into peripheral circulation, the use of G-CSF and the granulocyte-macrophage colony-stimulating factor has recently been reported as a clinical application of stem cell therapy[18,19]; however, the effect of M-CSF treatment on cardiac dysfunction and remodeling after permanent MI has not been entirely understood.

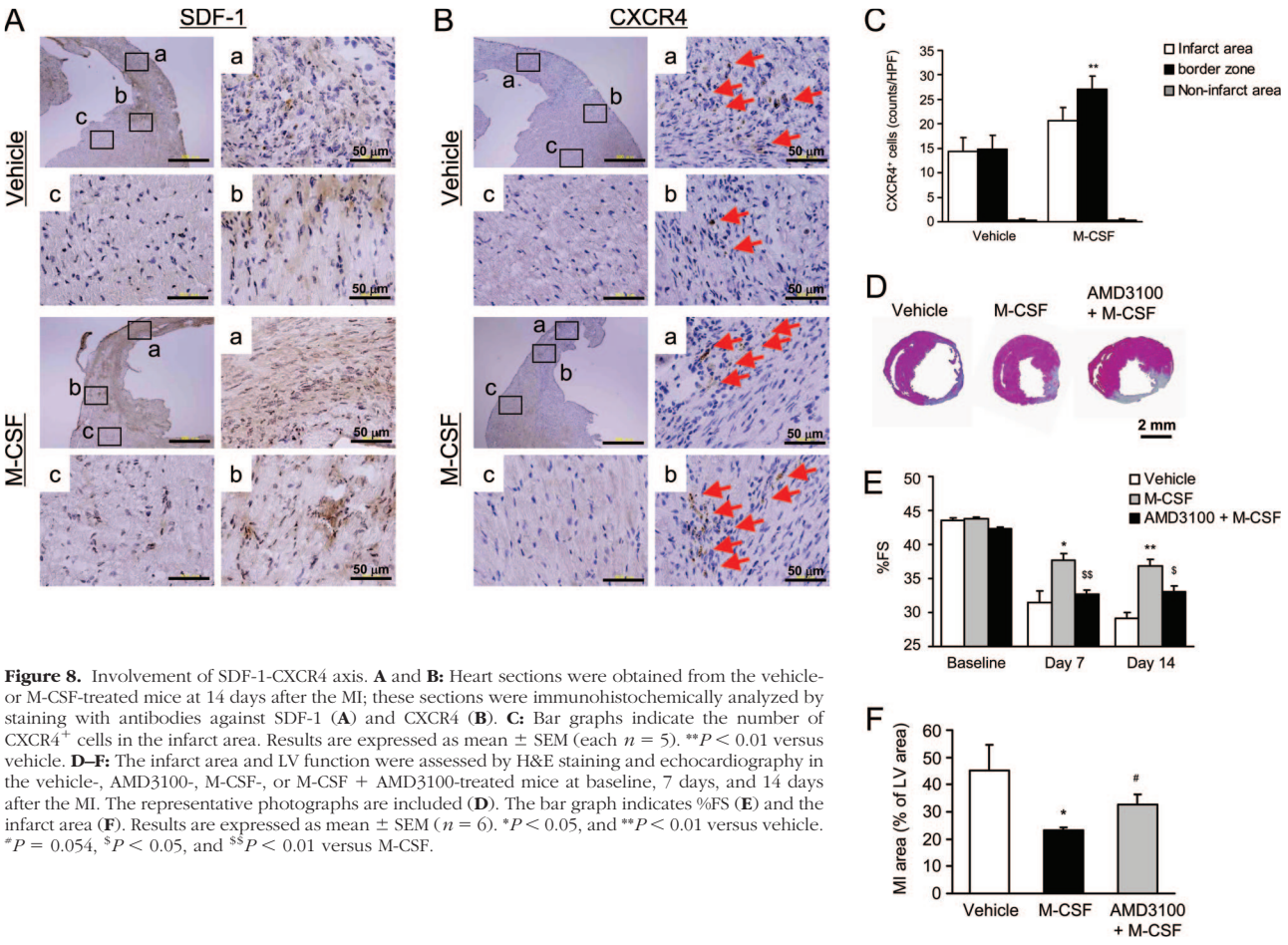

Figure 8. Involvement of SDF-1-CXCR4 axis. **A** and **B:** Heart sections were obtained from the vehicle- or M-CSF-treated mice at 14 days after the MI; these sections were immunohistochemically analyzed by staining with antibodies against SDF-1 (**A**) and CXCR4 (**B**). **C:** Bar graphs indicate the number of $CXCR4^+$ cells in the infarct area. Results are expressed as mean ± SEM (each $n = 5$). $^{**}P < 0.01$ versus vehicle. **D–F:** The infarct area and LV function were assessed by H&E staining and echocardiography in the vehicle-, AMD3100-, M-CSF-, or M-CSF + AMD3100-treated mice at baseline, 7 days, and 14 days after the MI. The representative photographs are included (**D**). The bar graph indicates %FS (**E**) and the infarct area (**F**). Results are expressed as mean ± SEM ($n = 6$). $^{*}P < 0.05$, and $^{**}P < 0.01$ versus vehicle. $^{\#}P = 0.054$, $^{\$}P < 0.05$, and $^{\$\$}P < 0.01$ versus M-CSF.

We clearly demonstrated that M-CSF treatment improved LV dysfunction, reduced the infarct size, and improved LV remodeling after permanent MI. Recently, Yano et al[20] reported that M-CSF treatment attenuated LV dysfunction after myocardial ischemia-reperfusion in rats; however, M-CSF had no effects on the infarct size, infarct transmurality, and the number of factor VIII-positive vessels in the infarct and noninfarct myocardium. In their study,[20] because M-CSF treatment increased TGF-β1 expression and the collagen content in the myocardium, they speculated that the beneficial effect of M-CSF was mediated through the acceleration of the myocardial repair processes. Although the reason for the discrepancy in the effect of M-CSF is unclear, there are a number of differences between the pathophysiology of permanent MI and ischemia-reperfusion injury.[21–23] Reperfusion releases a large excess of oxygen-derived free radicals and produces "reperfusion injury." Inflammatory responses such as the infiltration of neutrophils and macrophages are much stronger in the reperfused heart than in the infarct heart. Because the inflammatory response after MI is determinative for tissue healing,[23] the processes involved in myocardial healing, such as collagen deposition, are accelerated in the reperfused heart. Furthermore, reperfusion enhances neovascularization to a greater extent in the reperfused heart than in the infarct heart. Thus, we postulate that although M-CSF has beneficial effects on the repair processes of both permanent MI and ischemia-reperfusion, its mechanism of action might differ between these two conditions.

Effect of M-CSF Treatment on Macrophage Infiltration and Neovascularization

We demonstrated that M-CSF treatment increased macrophage infiltration and endothelial cell density after the MI. Monocytes/macrophages have been shown to promote the healing and repair processes of MI by several mechanisms. Macrophages produce cytokines and growth factors, which influence the process of myocardial healing.[24] In addition, macrophages may regulate extracellular matrix metabolism through the synthesis of matrix metalloproteinases and their inhibitors.[25] Thus, M-CSF-induced macrophage infiltration might play a role in the post-MI healing process. Previous reports showed that myofibroblasts are the predominant source of collagen and that TGF-β1 acts as a key mediator for myofibroblast differentiation during wound healing by regulating α-SMA expression.[23,26] Using a rat model of myocardial ischemia-reperfusion, Yano et al[20] recently reported that M-CSF treatment increased TGF-β1 expression and collagen content. However, in our study, M-CSF treatment did not increase myofibroblast accumulation and the expression of colla-

gen and TGF-β1 in the infarct area. Interestingly, M-CSF accelerated the *in vitro* differentiation of cardiac fibroblasts, peripheral blood cells, and bone marrow-derived cells. Furthermore, M-CSF decreased hypoxia-reoxygenation-induced apoptosis in cultured cardiomyocytes, although there was no difference in the number of apoptotic cells in the heart after MI between the vehicle- and M-CSF-treated mice. Although the reason for the discrepancy between *in vitro* and *in vivo* experiments is currently unclear, further investigation is required to elucidate the precise mechanisms underlying the beneficial effect of M-CSF. Taken together, our findings suggest that in a permanent MI model, the beneficial effect of M-CSF might at least in part depend on macrophage infiltration and neovascularization.

Recent evidence indicates that monocytes/macrophages promote neovascularization in ischemic tissues through several possible mechanisms. First, recent reports demonstrated that monocytes/macrophages produce matrix metalloproteinase-dependent tunnels and directly promote neovascularization.[1,27,28] Second, bone marrow-derived cells of monocytic lineage are suggested to function as EPCs and participate in the neovascularization of ischemic tissues.[2,3] In our study, M-CSF treatment increased the Mac-1^+/CXCR4^+ cells but not the CD34^+/Flk-1^+ cells (ordinary EPC marker) in peripheral circulation after the MI. In this regard, Harraz et al[2] reported that CD34^- angioblasts are a subset of CD14^+ monocytic cells and that these monocytes have the potential to transdifferentiate into endothelial cells; this suggests that EPCs derived from monocytic cells might have other surface markers.

There are several reports describing the role of SDF-1-CXCR4 axis in neointimal formation after vascular injury. Weber and his colleagues[29,30] reported that the SDF-1-CXCR4 axis contributed to the recruitment of bone marrow-derived smooth muscle progenitor cells and neointimal formation after vascular injury in apoE$^{-/-}$ mice. Zhang et al[31] also reported that the SDF-1-CXCR4 axis contributed to neointimal formation after the ligation of carotid artery in endothelial nitric-oxide synthase-deficient mice. Furthermore, we recently reported that M-CSF treatment accelerated neointimal formation after vascular injury via the SDF-1-CXCR4 axis.[32] These investigations suggest that the CXCR4^+ cells act as smooth muscle progenitor cells. In contrast, Walter et al[33] reported that impaired CXCR4 signaling contributes to the reduced neovascularization capacity of EPCs, suggesting that the CXCR4^+ cells function as EPCs in ischemic tissue. Furthermore, several studies demonstrated that bone marrow-derived CXCR4^+ cells promote neovascularization in ischemic tissue by the release of angiogenic factors.[34,35] Thus, we speculate that M-CSF-mobilized monocytic CXCR4^+ cells are retained by SDF-1 and accelerate neovascularization in the infarct area. Taken together, we postulate that the CXCR4^+ cells have the potential to function as both EPCs and smooth muscle progenitor cells according to the circumstances, and the SDF-1-CXCR4 system may contribute to the pathogenesis of cardiovascular diseases.

Role of the SDF-1-CXCR4 Axis in the Pathophysiology of MI

We demonstrated that M-CSF increased the CXCR4^+ cells in peripheral circulation, whereas MI induced SDF-1 expression in the infarct area. The mobilized CXCR4^+ cells were recruited to the infarct myocardium, and they interacted with SDF-1. The inhibitory effect of AMD3100 indicates the contribution of the SDF-1-CXCR4 axis to the beneficial effect of M-CSF. Interestingly, recent investigations demonstrated that the AMD3100 treatment rapidly mobilizes CD34^+ hematopoietic stem cells from the bone marrow into peripheral circulation[36] and that G-CSF combined with single injection of AMD3100 promoted angiogenesis in a murine model of hindlimb ischemia.[37] In our previous study,[32] however, continuous AMD3100 infusion had no effect on the re-endothelialization after vascular injury; this suggests that a continuous CXCR4 inhibition abrogates the chemotactic activity of SDF-1 and homing of CXCR4^+ cells to the SDF-1-expressing site. Supporting this, a recent study demonstrated that CXCR4^+ cells could not accumulate at the SDF-1-expressing site in animals harboring an osmotic pump releasing AMD3100.[35]

Several previous studies demonstrated that the SDF-1-CXCR4 axis participated in the neovascularization of ischemic tissues.[33,38] Consistent with our finding, by using a rabbit model of myocardial ischemia-reperfusion, Misao et al[39] very recently reported that the SDF-1-CXCR4 axis might be responsible for the G-CSF-induced improvement of LV dysfunction. Taken together, these findings suggest that the SDF-1-CXCR4 axis plays a crucial role in the beneficial effect of M-CSF in MI. Further studies are required to elucidate its precise role of the SDF-1-CXCR4 axis in the pathophysiology of MI.

Conclusion

We demonstrated that M-CSF treatment reduced infarct area and scar formation and improved LV dysfunction and remodeling after MI through the recruitment of CXCR4^+ cells into the infarct myocardium by the activation of SDF-1-CXCR4 axis. These findings suggest that M-CSF has a therapeutic potential for MI and that the SDF-1-CXCR4 axis could be new target for the treatment of ischemic heart diseases.

Acknowledgments

We thank Junko Nakayama, Tomoko Hamaji, and Kazuko Misawa for excellent technical assistance, Shinya Suzu (Kumamoto University, Kumamoto, Japan) for valuable suggestions, and Muneo Yamada (Morinaga Milk Industry Co. Ltd.) for providing M-CSF and anti-M-CSF antibody.

References

1. Schmeisser A, Garlichs CD, Zhang H, Eskafi S, Graffy C, Ludwig J, Strasser RH, Daniel WG: Monocytes coexpress endothelial and macrophagocytic lineage markers and form cord-like structures in Matrigel under angiogenic conditions. Cardiovasc Res 2001, 49:671–680
2. Harraz M, Jiao C, Hanlon HD, Hartley RS, Schatteman GC: CD34-blood-derived human endothelial cell progenitors. Stem Cells 2001, 19:304–312
3. Rehman J, Li J, Orschell CM, March KL: Peripheral blood "endothelial progenitor cells" are derived from monocyte/macrophages and secrete angiogenic growth factors. Circulation 2003, 107:1164–1169
4. Motoyoshi K: Biological activities and clinical application of M-CSF. Int J Hematol 1998, 67:109–122
5. Frangogiannis NG, Mendoza LH, Ren G, Akrivakis S, Jackson PL, Michael LH, Smith CW, Entman ML: MCSF expression is induced in healing myocardial infarcts and may regulate monocyte and endothelial cell phenotype. Am J Physiol 2003, 285:H483–H492
6. Misawa E, Sakurai T, Yamada M, Tamura Y, Motoyoshi K: Administration of macrophage colony-stimulating factor mobilized both $CD11b^+CD11c^+$ cells and $NK1.1^+$ cells into peripheral blood. Int Immunopharmacol 2004, 4:791–803
7. Werner N, Junk S, Laufs U, Link A, Walenta K, Bohm M, Nickenig G: Intravenous transfusion of endothelial progenitor cells reduces neointima formation after vascular injury. Circ Res 2003, 93:e17–e24
8. Morimoto H, Takahashi M, Izawa A, Ise H, Hongo M, Kolattukudy PE, Ikeda U: Cardiac overexpression of monocyte chemoattractant protein-1 in transgenic mice prevents cardiac dysfunction and remodeling after myocardial infarction. Circ Res 2006, 99:891–899
9. Yoshioka T, Takahashi M, Shiba Y, Suzuki C, Morimoto H, Izawa A, Ise H, Ikeda U: Granulocyte colony-stimulating factor (G-CSF) accelerates reendothelialization and reduces neointimal formation after vascular injury in mice. Cardiovasc Res 2006, 70:61–69
10. Kamiyoshi Y, Takahashi M, Yokoseki O, Yazaki Y, Hirose S, Morimoto H, Watanabe N, Kinoshita O, Hongo M, Ikeda U: Mycophenolate mofetil prevents the development of experimental autoimmune myocarditis. J Mol Cell Cardiol 2005, 39:467–477
11. Jia L, Takahashi M, Morimoto H, Takahashi S, Izawa A, Ise H, Iwasaki T, Hattori H, Wu KJ, Ikeda U: Changes in cardiac lipid metabolism during sepsis: the essential role of very low-density lipoprotein receptors. Cardiovasc Res 2006, 69:545–555
12. Harada M, Qin Y, Takano H, Minamino T, Zou Y, Toko H, Ohtsuka M, Matsuura K, Sano M, Nishi J, Iwanaga K, Akazawa H, Kunieda T, Zhu W, Hasegawa H, Kunisada K, Nagai T, Nakaya H, Yamauchi-Takihara K, Komuro I: G-CSF prevents cardiac remodeling after myocardial infarction by activating the Jak-Stat pathway in cardiomyocytes. Nat Med 2005, 11:305–311
13. Sugano Y, Anzai T, Yoshikawa T, Maekawa Y, Kohno T, Mahara K, Naito K, Ogawa S: Granulocyte colony-stimulating factor attenuates early ventricular expansion after experimental myocardial infarction. Cardiovasc Res 2005, 65:446–456
14. Virag JI, Murry CE: Myofibroblast and endothelial cell proliferation during murine myocardial infarct repair. Am J Pathol 2003, 163:2433–2440
15. Martin C, Burdon PC, Bridger G, Gutierrez-Ramos JC, Williams TJ, Rankin SM: Chemokines acting via CXCR2 and CXCR4 control the release of neutrophils from the bone marrow and their return following senescence. Immunity 2003, 19:583–593
16. Orlic D, Kajstura J, Chimenti S, Jakoniuk I, Anderson SM, Li B, Pickel J, McKay R, Nadal-Ginard B, Bodine DM, Leri A, Anversa P: Bone marrow cells regenerate infarcted myocardium. Nature 2001, 410:701–705
17. Asahara T, Masuda H, Takahashi T, Kalka C, Pastore C, Silver M, Kearne M, Magner M, Isner JM: Bone marrow origin of endothelial progenitor cells responsible for postnatal vasculogenesis in physiological and pathological neovascularization. Circ Res 1999, 85: 221–228
18. Zohlnhöfer D, Ott I, Mehilli J, Schomig K, Michalk F, Ibrahim T, Meisetschlager G, von Wedel J, Bollwein H, Seyfarth M, Dirschinger J, Schmitt C, Schwaiger M, Kastrati A, Schomig A: Stem cell mobilization by granulocyte colony-stimulating factor in patients with acute myocardial infarction: a randomized controlled trial. JAMA 2006, 295:1003–1010
19. Deng Z, Yang C, Deng H, Yang A, Geng T, Chen X, Ma A, Liu Z: Effects of GM-CSF on the stem cells mobilization and plasma C-reactive protein levels in patients with acute myocardial infarction. Int J Cardiol 2006, 113:92–96
20. Yano T, Miura T, Whittaker P, Miki T, Sakamoto J, Nakamura Y, Ichikawa Y, Ikeda Y, Kobayashi H, Ohori K, Shimamoto K: Macrophage colony-stimulating factor treatment after myocardial infarction attenuates left ventricular dysfunction by accelerating infarct repair. J Am Coll Cardiol 2006, 47:626–634
21. Kloner RA, Jennings RB: Consequences of brief ischemia: stunning, preconditioning, and their clinical implications: part 1. Circulation 2001, 104:2981–2989
22. Vandervelde S, van Amerongen MJ, Tio RA, Petersen AH, van Luyn MJ, Harmsen MC: Increased inflammatory response and neovascularization in reperfused vs. non-reperfused murine myocardial infarction. Cardiovasc Pathol 2006, 15:83–90
23. Frangogiannis NG, Smith CW, Entman ML: The inflammatory response in myocardial infarction. Cardiovasc Res 2002, 53:31–47
24. Weihrauch D, Arras M, Zimmermann R, Schaper J: Importance of monocytes/macrophages and fibroblasts for healing of microne-croses in porcine myocardium. Mol Cell Biochem 1995, 147:13–19
25. Lindsey ML: MMP induction and inhibition in myocardial infarction. Heart Fail Rev 2004, 9:7–19
26. Desmoulière A, Geinoz A, Gabbiani F, Gabbiani G: Transforming growth factor-β1 induces α-smooth muscle actin expression in granulation tissue myofibroblasts and in quiescent and growing cultured fibroblasts. J Cell Biol 1993, 122:103–111
27. Anghelina M, Krishnan P, Moldovan L, Moldovan NI: Monocytes/macrophages cooperate with progenitor cells during neovascularization and tissue repair: conversion of cell columns into fibrovascular bundles. Am J Pathol 2006, 168:529–541
28. Moldovan NI, Goldschmidt-Clermont PJ, Parker-Thornburg J, Shapiro SD, Kolattukudy PE: Contribution of monocytes/macrophages to compensatory neovascularization: the drilling of metalloelastase-positive tunnels in ischemic myocardium. Circ Res 2000, 87:378–384
29. Schober A, Knarren S, Lietz M, Lin EA, Weber C: Crucial role of stromal cell-derived factor-1α in neointima formation after vascular injury in apolipoprotein E-deficient mice. Circulation 2003, 108: 2491–2497
30. Zernecke A, Schober A, Bot I, von Hundelshausen P, Liehn EA, Mopps B, Mericskay M, Gierschik P, Biessen EA, Weber C: SDF-1α/CXCR4 axis is instrumental in neointimal hyperplasia and recruitment of smooth muscle progenitor cells. Circ Res 2005, 96:784–791
31. Zhang LN, Wilson DW, da Cunha V, Sullivan ME, Vergona R, Rutledge JC, Wang YX: Endothelial NO synthase deficiency promotes smooth muscle progenitor cells in association with upregulation of stromal cell-derived factor-1α in a mouse model of carotid artery ligation. Arterioscler Thromb Vasc Biol 2006, 26:765–772
32. Shiba Y, Takahashi M, Yoshioka T, Yajima N, Morimoto H, Izawa A, Ise H, Hatake K, Motoyoshi K, Ikeda U: M-CSF accelerates neointimal formation in the early phase after vascular injury in mice: the critical role of the SDF-1-CXCR4 system. Arterioscler Thromb Vasc Biol 2007, 27:283–289
33. Walter DH, Haendeler J, Reinhold J, Rochwalsky U, Seeger F, Honold J, Hoffmann J, Urbich C, Lehmann R, Arenzana-Seisdesdos F, Aicher A, Heeschen C, Fichtlscherer S, Zeiher AM, Dimmeler S: Impaired CXCR4 signaling contributes to the reduced neovascularization capacity of endothelial progenitor cells from patients with coronary artery disease. Circ Res 2005, 97:1142–1151
34. Jin DK, Shido K, Kopp HG, Petit I, Shmelkov SV, Young LM, Hooper AT, Amano H, Avecilla ST, Heissig B, Hattori K, Zhang F, Hicklin DJ, Wu Y, Zhu Z, Dunn A, Salari H, Werb Z, Hackett NR, Crystal RG, Lyden D, Rafii S: Cytokine-mediated deployment of SDF-1 induces revascularization through recruitment of $CXCR4^+$ hemangiocytes. Nat Med 2006, 12:557–567
35. Grunewald M, Avraham I, Dor Y, Bachar-Lustig E, Itin A, Jung S, Chimenti S, Landsman L, Abramovitch R, Keshet E: VEGF-induced adult neovascularization: recruitment, retention, and role of accessory cells. Cell 2006, 124:175–189
36. Broxmeyer HE, Orschell CM, Clapp DW, Hangoc G, Cooper S, Plett PA, Liles WC, Li X, Graham-Evans B, Campbell TB, Calandra G, Bridger G, Dale DC, Srour EF: Rapid mobilization of murine and

human hematopoietic stem and progenitor cells with AMD3100, a CXCR4 antagonist. J Exp Med 2005, 201:1307–1318
37. Capoccia BJ, Shepherd RM, Link DC: G-CSF and AMD3100 mobilize monocytes into the blood that stimulate angiogenesis in vivo through a paracrine mechanism. Blood 2006, 108:2438–2445
38. Yamaguchi J, Kusano KF, Masuo O, Kawamoto A, Silver M, Murasawa S, Bosch-Marce M, Masuda H, Losordo DW, Isner JM, Asahara T: Stromal cell-derived factor-1 effects on ex vivo expanded endothelial progenitor cell recruitment for ischemic neovascularization. Circulation 2003, 107:1322–1328
39. Misao Y, Takemura G, Arai M, Ohno T, Onogi H, Takahashi T, Minatoguchi S, Fujiwara T, Fujiwara H: Importance of recruitment of bone marrow-derived $CXCR4^{+}$ cells in post-infarct cardiac repair mediated by G-CSF. Cardiovasc Res 2006, 71:455–465